THE JOURNAL OF PHYSICAL CHEMISTRY A

Article

Cite This: J. Phys. Chem. A 2018, 122, 130−139

pubs.acs.org/JPCA

The Forbidden $1^1B_u^-$ Excited Singlet State in Peridinin and Peridinin Analogues

Jordan A. Greco, Nicole L. Wagner, Harry A. Frank, and Robert R. Birge*

Department of Chemistry, University of Connecticut, 55 North Eagleville Road, Storrs, Connecticut 06269-3060, United States

ABSTRACT: Theoretical studies have predicted the presence of a forbidden $1^1B_u^-$ state in proximity to the strongly allowed $1^1B_u^+$ excited state in polyenes and carotenoids. The $1^1B_u^-$ state is invariably predicted to have a very low oscillator strength, which precludes direct optical spectroscopic assignment. We report here a direct UV−vis optical spectroscopic feature assigned to the $1^1B_u^-$ state of S-2-peridinin, a synthetic analogue of the naturally occurring carotenoid, peridinin. The shift of the ground state dipole of S-2-peridinin compared to natural peridinin enhances the oscillator strength of absorption from the ground state to the $1^1B_u^-$ state by 2 orders of magnitude relative to peridinin. It is postulated that this is due to a quadrupolar electrostatic field generated from the more central location of the lactone ring along the polyene chain in S-2-peridinin. MNDO-PSDCI and EOM-CCSD calculations provide a theoretical basis for this assignment and explain the unique properties of the $1^1B_u^-$ state and why the transition from the ground state to this state has such a low oscillator strength in most other polyenes and carotenoids.

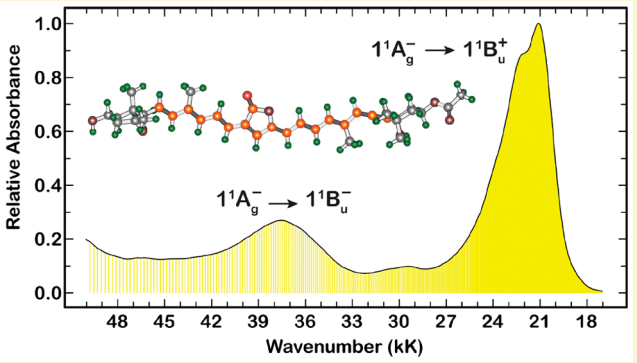

INTRODUCTION

Linear π-electron conjugated molecules are not only exploited by nature in the profoundly important processes of photosynthesis and vision,[1−3] but they have also provided an important testing ground for the development of modern quantum mechanics and molecular orbital (MO) theory.[4] Many of their photophysical properties can be traced to the fact that long chain linear polyenes have C_{2h} symmetry with a ground (S_0) state characterized by the $^1A_g^-$ irreducible representation[4,5] and a strongly allowed transition from this state to a $^1B_u^+$ excited state, which turns out not to be the lowest-lying excited state.[4−10] It was the pioneering discovery of a transition to a lower-lying optically forbidden $^1A_g^-$ state in diphenyloctatetraene by Hudson and Kohler[11] that produced a paradigm shift in our understanding of the energy ordering of polyene excited states.[4,9] Schulten and Karplus[9] provided a theoretical rationale for the experimental findings by including both singly and doubly excited states in a quantum computational analysis involving configuration interaction (CI). Their computations revealed that a low-lying $^1A_g^-$ state was predicted to lie below the $^1B_u^+$ state for linear polyenes with four or more carbon−carbon double bonds, N. Their analysis also predicted the presence of other low-lying excited singlet states, including a $^1B_u^-$ state, in polyenes with $N \geq 4$,[9,12−14] but spectroscopic evidence for the presence of this state in polyenes or carotenoids has remained controversial.

The $1^1B_u^-$ state is predicted by MO theory to lie above the strongly allowed $1^1B_u^+$ state for polyenes having $N < 12$ conjugated double bonds and below it for those having $N > 12$.[15,16] Regardless of the relative position of the $1^1B_u^-$ state within the excited state manifold, transitions to and from this state and the ground, S_0 ($1^1A_g^-$) state are strictly forbidden in linear polyenes. This manifests itself experimentally by such a low oscillator strength for most polyenes and carotenoids that the observation via UV−vis spectroscopy is exceedingly difficult. Moreover, a transition from the ground state to the $1^1B_u^-$ state is symmetry-forbidden according to both one-photon and two-photon selection rules for molecules belonging to the C_{2h} symmetry point group,[15] and due to low configurational overlap with observed states,[17] this transition does not gain significant intensity from conformational distortions that reduce the molecular symmetry.[9,13,14,16,17] Although evidence for the $1^1B_u^-$ state has been reported from pump−probe,[18−21] resonance Raman,[22−26] and two-photon polarization[27] spectra, these methods have led to tentative and controversial assignments.[28]

The subject of the present study is peridinin, a highly substituted carotenoid found in dinoflagellates, which is responsible for transferring absorbed light energy to chlorophyll *a* to facilitate photosynthetic growth by the organisms.[1,29−31] The structure of peridinin (Figure 1) contains several symmetry-breaking moieties, including a central lactone ring in conjugation with the polyene, as well as complex end groups. Polyene and carotenoid literature has generally adhered to an excited state labeling scheme based on idealized C_{2h} symmetry, even when molecular structures, like peridinin, show this

Received: October 9, 2017
Revised: December 1, 2017
Published: December 4, 2017

DOI: 10.1021/acs.jpca.7b10001
J. Phys. Chem. A 2018, 122, 130−139

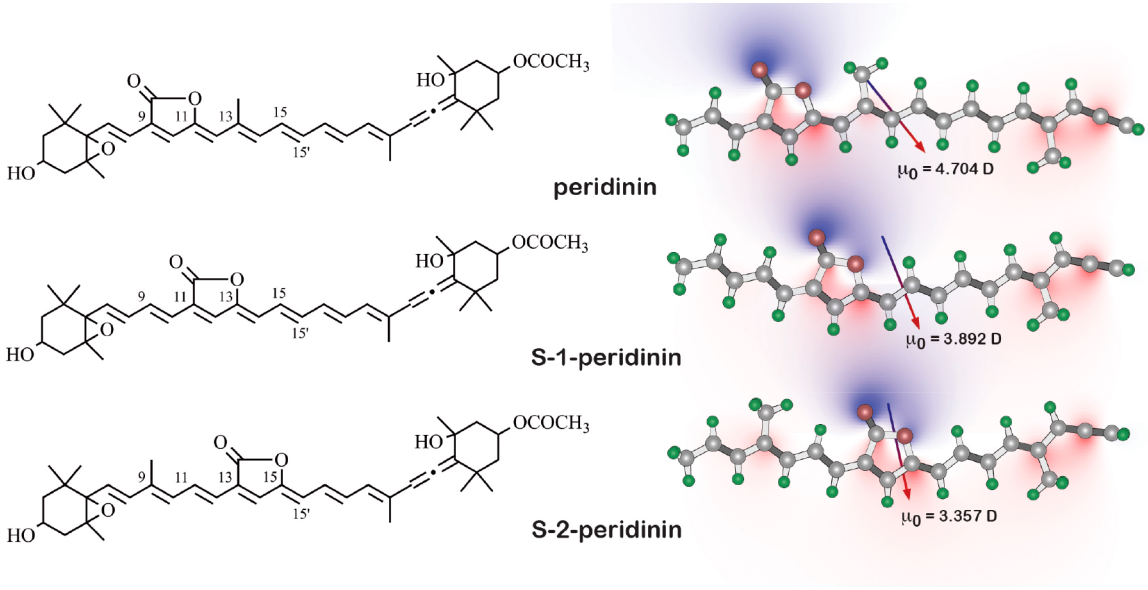

Figure 1. Structures of peridinin and the two lactone ring shifted variants are shown on the left. The corresponding truncated models used in some of the theoretical calculations are shown on the right. The models include the full polyene chain and the lactone ring, and because these models have C_s symmetry, higher levels of theory are possible. The background colors in the figures at right indicate regions of intrinsic excess negative (blue) and positive (red) charge associated with the presence of the lactone ring. The arrows show the direction of the ground-state dipole moment, the magnitude of which is displayed below the arrowhead.

assumption to be approximate. This scheme is justified because the substituted molecules tend to retain many of the spectroscopic characteristics of the polyene models with C_{2h} symmetry. However, specific symmetry-breaking features have been shown to deviate from the selection rules typically observed for molecules belonging to this point group. Recently, we reported the direct observation of absorption between the ground S_0 ($1^1A_g^-$) state and the low-lying S_1 ($2^1A_g^-$) excited state for the peridinin analogue, deoxyperidinin.[32] However, direct observation of a transition from the S_0 ($1^1A_g^-$) state to the $1^1B_u^-$ excited state via steady-state absorption spectroscopy carried out on carotenoids or polyene systems has remained elusive and has not yet been reported.

The photophysics of carotenoids are typically described within the framework of the three-level system originated for polyenes, and alluded to above, in which photoexcitation into the S_2 ($1^1B_u^+$) state leads to subsequent decay to the S_1 ($2^1A_g^-$) state in ∼100 fs and then back to the ground S_0 ($1^1A_g^-$) state in anywhere from one to a few hundred picoseconds, depending on N. The larger the value of N, the slower the rate of decay of the S_1 state, and this has been rationalized using the energy gap law for radiationless transitions.[33−35] However, the internal conversion decay rate from S_2 to S_1 was found to decrease with increasing energy gap between the two states,[36,37] which is in disagreement with the prediction of the energy gap law. This observation strongly suggests the presence of an intermediate "dark" state between S_1 and S_2 that can modulate the lifetime of the S_2 state depending on its position.[37] It has been argued that this intermediate state is involved in carotenoid-to-bacteriochlorophyll energy transfer in light-harvesting complexes of photosynthetic bacteria.[38] Importantly, some researchers have suggested that the involvement of this dark state in light-harvesting explains the disparity between the observed efficiency of this process and the calculated efficiency, which is less than half of the experimental value when only considering a three-level system.[39−43]

Ultrafast time-resolved transient absorption spectroscopic experiments carried out by Zhang et al.[20] and Cerullo et al.[18] suggested that a dark intermediate state, termed S_x, which was needed to account for their observations, was possibly the $1^1B_u^-$ state populated during the decay between S_2 and S_1 for carotenoids having $N \geq 9$. Indeed, the assignment of the dark intermediate state to a $1^1B_u^-$ state would be consistent with the computational models for polyenes advanced by Tavan and Schulten,[15] and additional quantum mechanical calculations support this view.[16,17,22,44−50] Also, spectroscopic bands in the near-IR (800−950 nm)[51−53] or visible (∼600 nm)[54−56] regions of the transient absorption spectra for various carotenoids were assigned to the $1^1B_u^-$ state in subsequent reports. More recently, Ostroumov et al.[19,57] employed two-dimensional electronic spectroscopy and argued that the S_x state is the $1^1B_u^-$ state and that it electronically couples with both the $1^1B_u^+$ state of the carotenoid and the Q_x band of bacteriochlorophyll via the Herzberg−Teller mechanism.[58−60]

Despite the progress made in probing the excited state manifolds of polyenes and the enticing assignments of recent work, a consensus has not been reached on the character and function of the S_x intermediate.[28] Recent analyses of the dynamics of carotenoid excited states by various ultrafast time-resolved spectroscopic methods have suggested that the S_x state is more appropriately attributed to either the $3^1A_g^-$ state,[25,51,61] a hot S_1 state,[62−66] a vibrationally excited S_0 band (i.e., the S* state),[67] or a different potential energy minimum of the S_2 state induced by torsional motion and bond-length alternation.[68−70] Other reports claim that there is in fact no observable intermediate present in the relaxation pathway from S_2 to S_1.[71−76] Fleming et al.[77] recently suggested that the dynamics between S_2 and S_1 are governed instead by a decay pathway through the conical intersection of the two states. This conclusion may further be supported by the excited state properties described in this investigation, in which the $1^1B_u^-$

DOI: 10.1021/acs.jpca.7b10001
J. Phys. Chem. A 2018, 122, 130−139

state is shown to lie above the $1^1B_u^+$ state for peridinin and related analogues.

The work presented here will take advantage of systematic alterations in the structure of peridinin to affect a profound influence on the observation and behavior of the optically forbidden $1^1B_u^-$ state and, in doing so, will allow a re-examination of the interpretations of the excited dynamics of the S_2 state and the dark states of carotenoids. This present work reports the direct optical observation of the $1^1B_u^-$ state in a synthetic analogue of peridinin. The key to the findings was made possible by the fact that the ground state dipole moment of the peridinin chromophores is shifted when the lactone ring is systematically moved toward the center of the all-*trans* polyene chain. With respect to naturally occurring peridinin, S-1- and S-2-peridinin have the lactone ring positioned two and four carbon atoms closer, respectively, to the allenic region of the chromophore (Figure 1). This series of peridinin analogues has been previously studied to investigate the effect of molecular symmetry on the lifetime of the S_1 state and the factors influencing the formation of the now well-established intramolecular charge transfer (ICT) state present in carbonyl-containing carotenoids.[78] Here, it is shown that one of these chromophores, S-2-peridinin, has the intensity of the S_0 ($1^1A_g^-$) $\rightarrow$ $1^1B_u^-$ transition enhanced by an order of magnitude relative to peridinin, S-1-peridinin, and other carotenoids and polyenes. It is postulated that the oscillator strength of this transition is enhanced via a quadrupolar electrostatic field within the polyene chromophore. MNDO-PSDCI and EOM-CCSD calculations provide a theoretical basis for this assignment and help to explain the unique properties of the $1^1B_u^-$ state and why a transition from the ground state to this state has such a low oscillator strength for most polyenes and carotenoids.

MATERIALS AND METHODS

Sample Preparation and Spectroscopy. The molecules investigated in this study are shown in Figure 1 along with the model chromophores that reproduce the polyene segment without the complex end groups. Peridinin was extracted from thylakoid membranes of *Amphidinium carterae* as previously described.[79] S-1-Peridinin and S-2-peridinin were synthesized by the group of Prof. Shigeo Katsumura at Kwansei Gakuin University[80] and were stored as dried crystals. All pigments were purified as previously described.[78] Steady-state absorption spectra were measured on a Varian Cary 5000 UV–vis spectrometer.

Theoretical Methods. All *ab initio* and density functional calculations were carried out by using Gaussian 09.[81] Ground state density functional calculations on the full and truncated chromophores used the B3LYP functional and the 6-31G(d) basis set. The molecules were optimized in solvent where indicated using the polarizable continuum model (PCM).[82−84] The truncated molecules shown in Figure 1 have been previously implemented as a means to simplify peridinin to the polyene backbone and to use a more tractable model for excited state calculations.[85,86] In this study, we explored both forms of the chromophores to study the influence of the end groups on the formation of the $1^1B_u^-$ state.

Excited state calculations were carried out by using a variety of MO methods for comparative purposes. Modified neglect of differential overlap with partial single- and double-CI (MNDO-PSDCI) methods[27,87] were used to explore the oscillator strengths and transition energies of the low-lying singlet states. This semiempirical method includes single and double excitations within the π system and has been useful in understanding the electronic properties of long chain polyenes and carotenoids.[17,85,88] The standard Austin Model 1 (AM1) parametrization was used, including Mataga repulsion integrals (*rijm* = 2) and identical π and σ electron mobility constants of 1.7 (*pimc* = *sigmc* = 1.7).[27,87] All MNDO-PSDCI transition energies are relative to the uncorrelated ground state.[12] The MNDO-PSDCI calculations were carried out using our own program, which is freely available upon request by contacting R.R.B. (rbirge@uconn.edu).

Equation-of-motion coupled-cluster with singles and doubles (EOM-CCSD) methods were also employed, using an active space of the 22 highest energy filled and the 22 lowest energy virtual MOs, unless otherwise indicated.[89] Excited state properties were calculated relative to either the second- or third-order Møller–Plesset (MP2 or MP3) ground state,[90] and the calculations used the double-ζ D95 basis set.[91] In addition, the PCM solvation approach was used to explore the effect of solvent on the excited state properties.[82−84]

RESULTS AND DISCUSSION

Spectroscopic Analysis. The absorption spectra of peridinin, S-1-peridinin, and S-2-peridinin in *n*-hexane are shown in Figure 2 (top). This figure also presents the difference spectra of the S-1- and S-2-peridinins versus the native peridinin chromophore in the middle and bottom panels, respectively. Band maxima tentatively assigned to individual excited states are marked with solid circles, and the band centered at ~35 kK (~285 nm, ~4.35 eV) is the target of this investigation. We assign this band to the $1^1B_u^-$ state and note that this band shifts to the blue (~38 kK, 263 nm, 4.71 eV) and is more intense in S-2-peridinin. The position of the $1^1B_u^-$ state above the strongly allowed $1^1B_u^+$ state is consistent with the observations by Tavan and Schulten[14,15] for linear polyenes with $N \leq 12$ (N = 7 for peridinin, S-1-peridinin, and S-2-peridinin). The absorption spectra of peridinin, S-1-peridinin, and S-2-peridinin in acetonitrile are shown in Figure 3. The band at ~35 kK (~285 nm, ~4.35 eV) displays the same characteristics as observed in *n*-hexane with a maximum intensity and transition energy in S-2-peridinin, in addition to a minor blue-shift. This spectroscopic feature has a higher relative intensity in acetonitrile than in *n*-hexane.

Theoretical Assignment of the $1^1B_u^-$ State. Both the full and the truncated structures of the chromophores (Figure 1) were investigated in order to examine the influence of the end groups on the calculated electronic transitions. The level ordering and spectroscopic properties of the five lowest-lying excited singlet states are predicted by MNDO-PSDCI and EOM-CCSD procedures to be identical for both groups of chromophores provided the feature at ~35 kK (~285 nm, ~4.35 eV) is assigned to the $1^1B_u^-$ state. Thus, both the *ab initio* and semiempirical calculations show that the end groups do not have a significant effect on the low-lying transitions. Overall, the EOM-CCSD procedures on the full chromophores best reproduce the experimental results and, hence, will form the primary basis for the analysis described below.

The EOM-CCSD calculations presented in Figure 4 were used to identify the third excited state (S_3) as the $1^1B_u^-$ state based on the increase in oscillator strength, the high degree of covalency, the diminished contribution from double excitations, and the relative position of the state known to be in close proximity to the $1^1B_u^+$ state. The results also predict that the transition from the ground state to the $1^1B_u^-$ state is very weak

DOI: 10.1021/acs.jpca.7b10001
J. Phys. Chem. A 2018, 122, 130−139

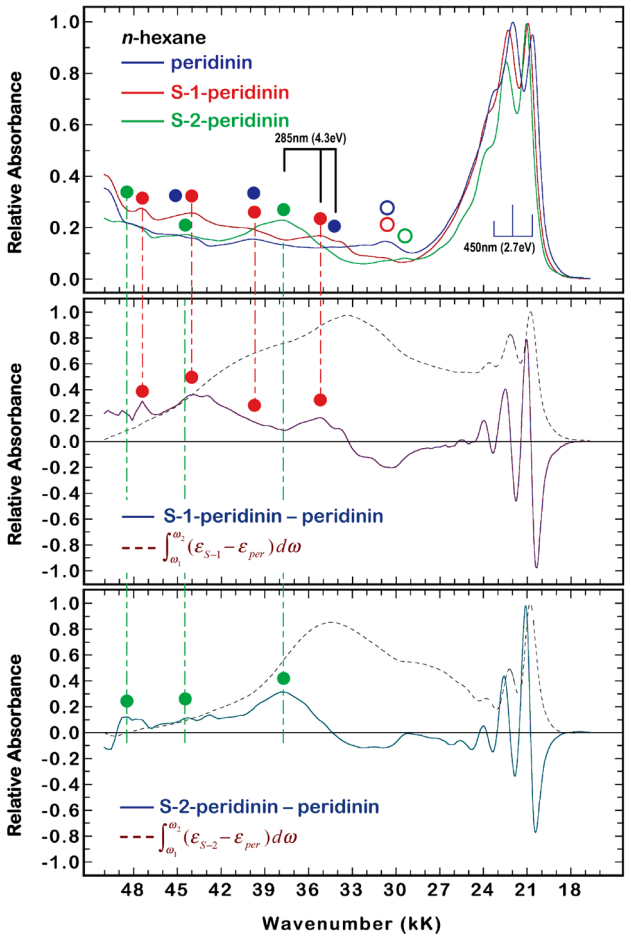

Figure 2. Absorption spectra (top) and difference spectra of peridinin, S-1-peridinin, and S-2-peridinin in *n*-hexane. The strongest band at 21 kK (1 kK = 1000 cm^{-1}) is assigned to the strongly allowed $1^1B_u^+$ state. The relatively strong band at 37 kK in S-2-peridinin is assigned to the $1^1B_u^-$ state. Selected higher energy states are marked using blue (peridinin), red (S-1-peridinin), and green (S-2-peridinin) dots. The open circles represent unassigned transitions that are likely not associated with the polyene framework. Note that the $1^1B_u^-$ state transition has virtually no intensity in peridinin, as predicted by the calculations. The difference spectra were generated by adjusting the intensity of all spectra in the 16−50 kK region to yield an identical integrated oscillator strength, as shown in the dashed line in the middle and bottom spectra.

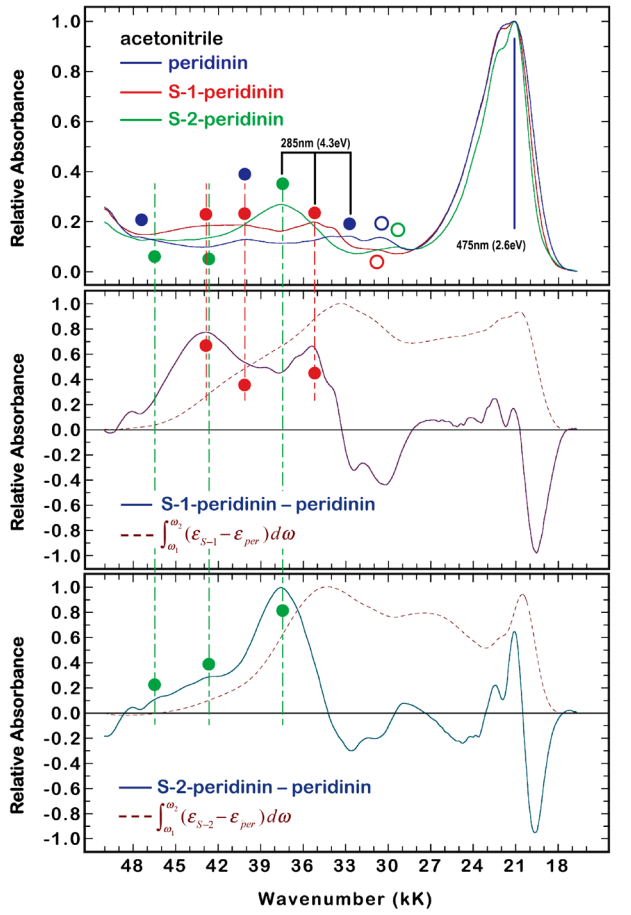

Figure 3. Absorption spectra and difference spectra of peridinin, S-1-peridinin, and S-2-peridinin in acetonitrile (ε = 32.613). Details of this analysis are as described in Figure 2.

in peridinin, gains intensity in S-1-peridinin, and has a relatively large oscillator strength of ~0.45 in S-2-peridinin. This trend is mirrored by the band assigned to the $1^1B_u^-$ state in the spectra of Figures 2 and 3. Note that the experimental spectra indicate that this feature is significantly more intense in acetonitrile than in *n*-hexane (Figures 2 and 3). However, an analysis of the band system using EOM-CCSD methods suggests that the intensity of the S_0 $(1^1A_g^-) \rightarrow 1^1B_u^-$ transition is roughly equal in *n*-hexane and acetonitrile. While the predicted effect of solvent is not in complete quantitative agreement with the experimental findings, the ratio of the oscillator strengths of the $1^1B_u^-$ and $1^1B_u^+$ state transitions is predicted to increase in acetonitrile and that difference is sufficient to explain the observed slight increase in the relative intensity of the $1^1B_u^-$ band. Moreover, the lack of quantitative agreement may also reflect the approximate nature of the PCM procedures.

It is worth pointing out that the calculations depicted in Figure 4 also suggest that the S_0 $(1^1A_g^-) \rightarrow 2^1A_g^-$ transitions for each molecule have oscillator strengths that are similar in magnitude to the S_0 $(1^1A_g^-) \rightarrow 1^1B_u^-$ transition in S-2-peridinin. Thus, one might ask why we are not observing the $2^1A_g^-$ state in the absorption spectra shown in Figures 2 and 3. There are two possibilities. First, the calculations indicate that the $2^1A_g^-$ state is separated, for example, by 0.29 eV from the $1^1B_u^+$ state in peridinin, whereas the $1^1B_u^-$ state is separated by 0.68 eV from the $1^1B_u^+$ state. The increased isolation of the $1^1B_u^-$ state from the strongly allowed $1^1B_u^+$ state is key to understanding why we can observe the $1^1B_u^-$ state as a separate band in S-2-peridinin. Second, we know from previous studies that both the $2^1A_g^-$ and $1^1B_u^+$ states are highly homogeneously broadened due to the presence of the lactone ring in peridinin. When the carbonyl in the lactone ring is replaced with a nonconjugated methylene group, the $1^1B_u^+$ vibronic structure becomes much sharper and the lowest-lying $2^1A_g^-$ state can be observed in a nonpolar glass at 77 K (see ref 32).

The most important observation from the excited state calculations is that there is no other excited singlet state predicted by the EOM-CCSD or the MNDO-PSDCI calculations other than the $1^1B_u^-$ state that even comes close to matching the observed behavior of the transition of interest within the experimental spectra. The theory provides a clear assignment based on level ordering and the effect of molecular properties on the transition energy and oscillator strength.

DOI: 10.1021/acs.jpca.7b10001
J. Phys. Chem. A 2018, 122, 130−139

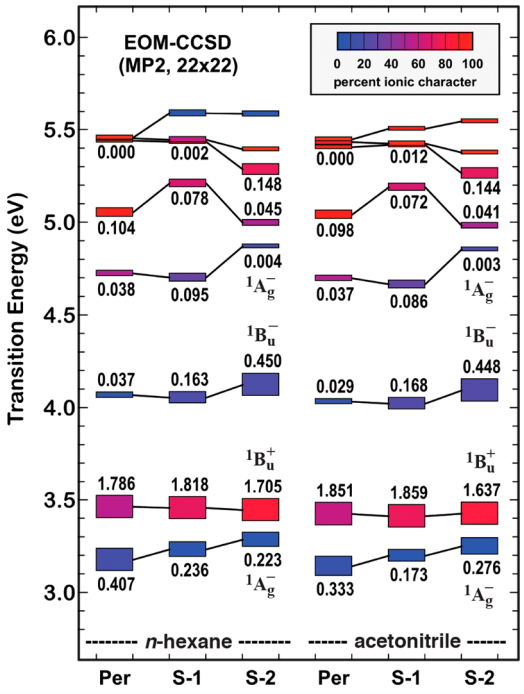

Figure 4. EOM-CCSD calculations on peridinin (Per), S-1-peridinin (S-1), and S-2-peridinin (S-2) in *n*-hexane (left) and acetonitrile (right). The EOM-CCSD calculations were carried out on the full molecules (including the end groups) using a window of 22 filled and 22 open MOs, and the transition energies and oscillator strengths were calculated relative to the MP2 ground state. The solvent was simulated by using PCM procedures. The symmetry labels are approximate and intended to provide qualitative assignments of the low-lying excited states. The height of each rectangle is proportional to the oscillator strength, and the percent covalent character is indicated by color with reference to the scale at the top right.

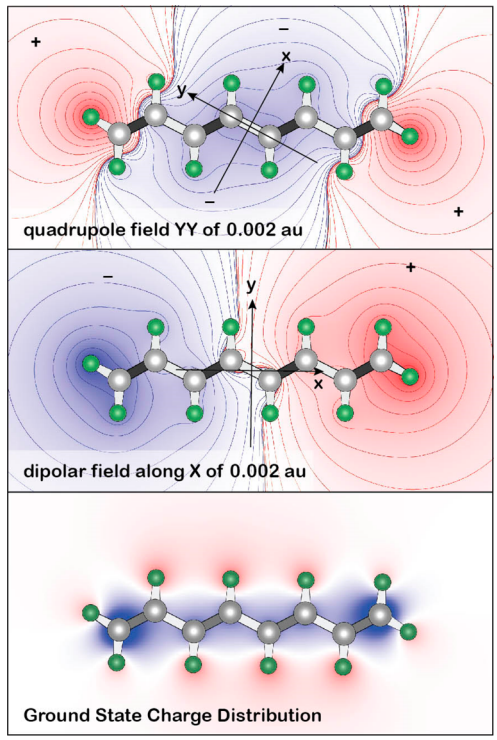

Figure 5. Effects of dipolar and quadrupolar fields on the ground state charge distributions of octatetraene. The charge maps in the top two panels are difference maps showing the change in the charge distribution associated with the applied field. A 0.002 au field equals 1.0284×10^9 V/m. The bottom panel depicts the relative Mulliken charges in the ground state, where red is positive and blue is negative.

What remains is to provide a perspective on why the S-2-peridinin analogue enhances the intensity of the $1^1B_u^-$ state by an unprecedented amount based on all the previous polyene studies.

Mechanism of $1^1B_u^-$ State Enhancement in S-2-Peridinin. We postulate that the unique properties of S-2-peridinin, as it pertains to an enhanced allowedness of the $1^1B_u^-$ state, is associated with the creation of a quadrupolar field by the charge distribution of the molecule. We arrived at this conclusion by a process of trial and error and the observation that an externally applied quadrupolar field reproduced the properties observed.

To explore this mechanism in more detail, we first examine the effect of dipolar and quadrupolar fields on a simple polyene, octatetraene. Calculations were run using various orientations of the induced charge distribution, and the effect of these fields on the polyene chain are shown in Figure 5. When the dipolar field is applied along the long axis of the polyene (x in Figure 5), the maximum impact is observed by creating a dipole moment directed along the *x*-axis. In contrast, the quadrupolar field is a higher order tensorial field that when applied along the central single bond moves charge symmetrically as shown in the top panel of Figure 5. The center of the polyene becomes more negative, and the ends become more positive, therefore yielding a positive YY field (Figure 5). If the field is reversed, the center becomes more positive and the ends become more negative. Thus, a quadrupolar field does not necessarily generate a dipole moment.

The effects of the dipolar and quadrupolar fields shown in Figure 5 on the low-lying excited singlet states of octatetraene are presented in Figures 6 and 7. The dipolar field mixes the lowest-lying $2^1A_g^-$ state with the nearby $1^1B_u^+$ state, transferring allowedness from the latter strongly allowed state into the zero-field forbidden $2^1A_g^-$ state. The sum of the oscillator strengths of these two states is, to a first approximation, invariant to the mixing process. A higher-order analysis, however, shows that some intensity is lost in the mixing process due to mixing of $1^1B_u^+$ state allowedness into much higher energy $^1A_g^-$ states. The amount of mixing is proportional to the polarizability of the polyene along the axis which the field is applied. Because the polarizability along the principal axis of the polyene (x in Figure 5, middle panel) is roughly 10 times higher than it is orthogonal to this axis, the effect of an applied field is roughly 10 times higher along the *x*-axis (compare X50 versus Y50 in Figure 6). For reference, the ordinate labels indicate the direction (X versus Y) and the magnitude of the field is given by the subsequent numbers in atomic units times 1000. Thus, X50 indicates a field of 0.005 au along the *x*-axis. A 0.005 au field equals 2.571×10^9 V/m. A key observation is that the $1^1B_u^-$ state remains largely unaffected by a dipolar field regardless of direction. This observation helps to explain why this state appears to be rigorously forbidden in both polar and nonpolar polyenes.

All of our theoretical methods predict a small $1^1B_u^-$ state oscillator strength in octatetraene under zero-field conditions [$f(1^1B_u^-$, MNDO-PSDCI) = 0.0023, $f(1^1B_u^-$, EOM-CCSD) = 0.0141]. The origin of the small oscillator strength is due to a breakdown of the pure covalency of the $1^1B_u^-$ state from the slight asymmetry of the single configurations, which do not

DOI: 10.1021/acs.jpca.7b10001
J. Phys. Chem. A 2018, 122, 130−139

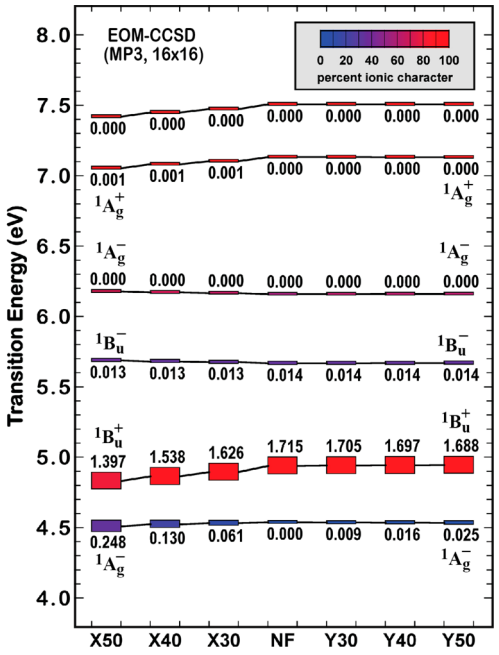

Figure 6. Effects of a dipolar field on the transition energies and oscillator strengths of the low-lying excited singlet states of octatetraene. The EOM-CCSD calculations were carried out using a window of 16 filled and 16 open MOs and the transition energies, and oscillator strengths were calculated relative to the MP3 ground state. The $1^1B_u^-$ state is the third excited state, and the oscillator strength and transition energy are largely invariant to the dipolar field. Note that a dipolar field along the main axis of the polyene mixes the $2^1A_g^-$ and $1^1B_u^+$ states (see Figure 5 for axis designation).

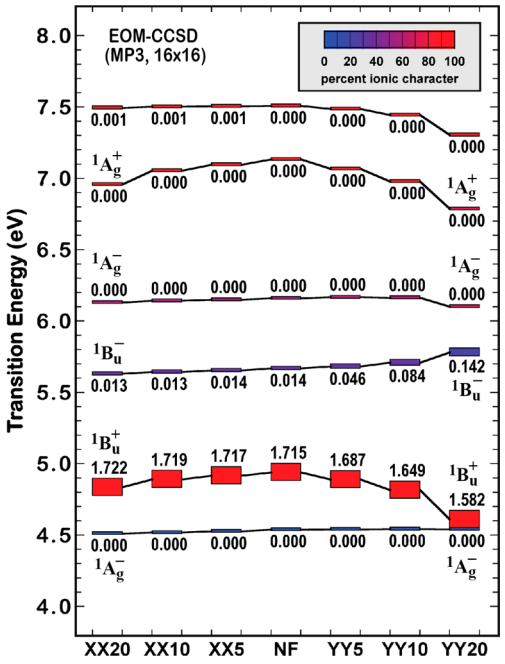

Figure 7. Effects of a quadrupolar field on the transition energies and oscillator strengths of the low-lying excited singlet states in octatetraene. The EOM-CCSD calculations were carried out using a window of 16 filled and 16 open MOs, and the transition energies and oscillator strengths were calculated relative to the MP3 ground state. The $1^1B_u^-$ state is the third excited state, and the oscillator strength is invariant to an XX quadrupolar field but enhanced significantly by a YY quadrupolar field (Figure 5, center panel). A key impact of the quadrupolar field is to mix the second excited $1^1B_u^+$ state with the third excited $1^1B_u^-$ state. Note that the sum of the oscillator strengths in these two states remains relatively constant. The lowest lying $2^1A_g^-$ excited state is largely unaffected by a quadrupolar field.

balance out perfectly due to mixing of doubles into the configurational description. Whether this asymmetry is a genuine feature of the polyene or a computational artifact remains a topic for further analysis. However, all theories that include σ MOs invariably predict a nonzero oscillator strength for the $1^1B_u^-$ state, even though the oscillator strength is so low that observation is made impossible by inhomogeneous broadening of neighboring states.

What is more interesting is the observation that conformational distortion does not generate significant oscillator strength in this excited state. A series of MNDO-PSDCI calculations on distorted, vibrationally hot, and *cis*-linkage conformations of octatetraene indicate that the oscillator strength of the $1^1B_u^-$ state transition is largely invariant to conformation and configuration. This near-conformational invariance of the $1^1B_u^-$ state oscillator strength has been noted before in studies on carotenoids[17] and long-chain polyenes.[16]

We propose that the central location of the lactone ring creates an effective quadrupolar field within the chromophore, shifting positive charge to the ends of the polyene and creating a region of negative charge near the center of the polyene chain. The result is demonstrated in the model chromophore shown in the bottom right of Figure 1. Note the coarse similarity of the latter charge distribution with that observed in the top panel of Figure 5. A quadrupolar field mixes the $1^1B_u^-$ and the $1^1B_u^+$ states effectively, as shown in Figure 7. This mixing transfers allowedness from the $1^1B_u^+$ state transition into that of the $1^1B_u^-$ state, while keeping the sum of the oscillator strengths nearly constant. For example, a YY quadrupolar field of 0.002 au (YY20 in Figure 7) transfers 0.13 units of oscillator strength into the $1^1B_u^-$ state, while the sum of the $1^1B_u^+$ and $1^1B_u^-$ state oscillator strengths remains ~1.72. Of equal importance to our assignment is the observation that the $1^1B_u^-$ state is blue-shifted by this field. The increase in both oscillator strength and transition energy of the $1^1B_u^-$ state is observed experimentally in the spectra shown in Figures 2 and 3 and in the EOM-CCSD calculations shown in Figure 4.

A quadrupolar field has no significant impact on the $2^1A_g^-$ state. Thus, although the $2^1A_g^-$ and the $1^1B_u^-$ states are highly covalent states, their response to external and internal fields is very different. We explore these surprising results in more detail below.

Configurational Analysis. The lowest three excited singlet states of peridinin and S-2-peridinin are examined with respect to EOM-CCSD configurational character in Figure 8. Single excitations are indicated using red vertical lines with the percent contribution of the excitation to the CI description shown inside the yellow circle. Double excitations are indicated using a pair of blue vertical lines with the percent contribution shown inside the yellow circle. Only excitations contributing 2% or more to the state description are shown, so these numbers do not necessarily add up to 100%.

Mixing between two excited states is evidenced in CI calculations by the presence of identical configurations in the description of the two states. Mixing of double excitations, however, does nothing to transfer allowedness because they do not interact with light. Such mixing is illustrated in Figure 8 by using blue lines to identify identical double configurations. Mixing involving single excitations can transfer allowedness

DOI: 10.1021/acs.jpca.7b10001
J. Phys. Chem. A 2018, 122, 130−139

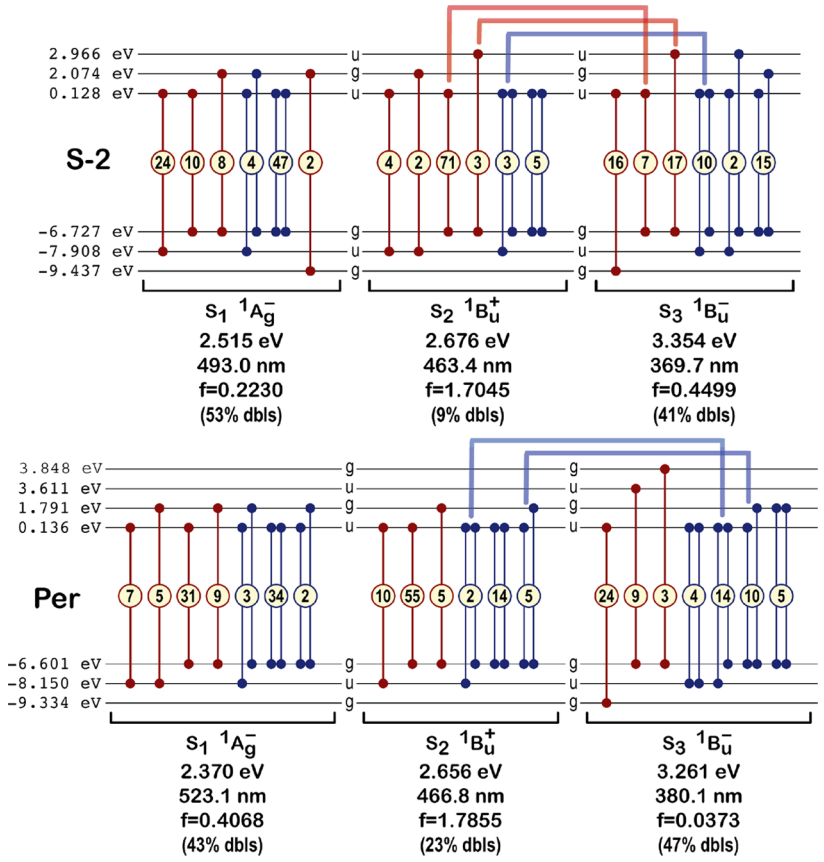

Figure 8. Configurational analysis of the lowest three excited singlet states of peridinin (Per) and S-2-peridinin (S-2) based on the EOM-CCSD calculations shown in Figure 4 for *n*-hexane. The principal mechanism of oscillator strength enhancement of the $1^1B_u^-$ state in S-2-peridinin is through intensity borrowing from the $1^1B_u^+$ state. The process is reflected in an overlap in the configurational properties of the two states and, in the case of intensity borrowing, an overlap in single excitations. Identical double excited configurations are marked with blue lines, and identical single excited configurations are marked with red lines.

from a canonical allowed state to a forbidden one. This effect is illustrated in Figure 8 using red lines to identify identical single configurations. The key observation is that $\langle 1^1B_u^-|H'|1^1B_u^+\rangle$ coupling via single excitations is unique to S-2-peridinin and is responsible for the pronounced intensity of the S_0 $(1^1A_g^-) \rightarrow 1^1B_u^-$ transition for this molecule.

CONCLUSIONS

Using analogues of peridinin with the lactone ring shifted toward the center of the polyene chain, we were able to observe directly the spectroscopic transition from the ground state to that of the of the forbidden $1^1B_u^-$ state. The dipole-shifted S-2-peridinin analogue displayed an observable band higher in energy than that associated with the strongly allowed $1^1B_u^+$ state, a position consistent with previous quantum mechanical analyses of long chain linear polyenes. Through a systematic theoretical treatment of the peridinin analogues and the unsubstituted octatetraene, we traced the origin of this spectroscopic feature to an intrinsic quadrupolar field of S-2-peridinin created by the central location of the lactone ring, which enhances the mixing of the forbidden $1^1B_u^-$ state with the strongly allowed $1^1B_u^+$ state. This result should inspire subsequent work on other symmetry-breaking long-chain polyenes and carotenoids in order to reveal the inherent quantum mechanical behavior and photophysics of these important molecules.

AUTHOR INFORMATION

Corresponding Author

*Phone 860-679-2558; Fax 860-486-2981; e-mail rbirge@uconn.edu (R.R.B.).

ORCID

Jordan A. Greco: 0000-0001-7582-9321

Notes

The authors declare no competing financial interest.

ACKNOWLEDGMENTS

We express our sincere gratitude to Shohei Hananoki, Shinji Hasegawa, Takayuki Kajikawa, and Shigeo Katsumura in the Department of Chemistry, Kwansei Gakuin University, 669-1337, Hyogo, Japan, for synthesizing the peridinin analogues used in our previously published spectroscopic investigations which inspired the present work. We also thank Amy M. LaFountain for providing the absorption spectra for this investigation. Work in the laboratory of R.R.B. was supported by grants from the National Institutes of Health (GM-34548) and the Harold S. Schwenk Sr. Distinguished Chair in Chemistry. Work in the laboratory of H.A.F. was supported by grants from the National Science Foundation (MCB-1243565) and the University of Connecticut Research Foundation.

DOI: 10.1021/acs.jpca.7b10001
J. Phys. Chem. A 2018, 122, 130−139

REFERENCES

(1) Polívka, T.; Frank, H. A. Molecular Factors Controlling Photosynthetic Light Harvesting by Carotenoids. *Acc. Chem. Res.* **2010**, *43*, 1125−1134.

(2) Koyama, Y.; Kuki, M.; Andersson, P. O.; Gillbro, T. Singlet Excited States and the Light-Harvesting Function of Carotenoids in Bacterial Photosynthesis. *Photochem. Photobiol.* **1996**, *63*, 243−256.

(3) Wald, G. The Molecular Basis of Visual Excitation. *Nature* **1968**, *219*, 800−808.

(4) Hudson, B.; Kohler, R. Linear Polyene Electronic Structure and Spectroscopy. *Annu. Rev. Phys. Chem.* **1974**, *25*, 437−460.

(5) Honig, B.; Dinur, U.; Birge, R. R.; Ebrey, T. G. The Isomer Dependence of Oscillator Strengths in Retinal and Related Molecules. *J. Am. Chem. Soc.* **1980**, *102*, 488−494.

(6) Becker, R.; Inuzuka, K.; Balke, D. Comprehensive Investigation of the Spectroscopy and Photochemistry of Retinals. I. Theoretical and Experimental Considerations of Absorption Spectra. *J. Am. Chem. Soc.* **1971**, *93*, 38−42.

(7) Birge, R. R.; Pierce, B. M. A Theoretical Analysis of the Two-Photon Properties of Linear Polyenes and the Visual Chromophores. *J. Chem. Phys.* **1979**, *70*, 165−178.

(8) Das, P. K.; Becker, R. S. Spectroscopy of Polyenes. 1. Comprehensive Investigation of Absorption Spectra of Polyenals and Polyenones Related to Visual Chromophores. *J. Phys. Chem.* **1978**, *82*, 2081−2092.

(9) Schulten, K.; Karplus, M. On the Origin of a Low-Lying Forbidden Transition in Polyenes and Related Molecules. *Chem. Phys. Lett.* **1972**, *14*, 305−309.

(10) Tallent, J. R.; Birge, J. R.; Zhang, C.-F.; Wenderholm, E.; Birge, R. R. Conformational Energetics and Excited State Level Ordering in 11-*cis* Retinal. *Photochem. Photobiol.* **1992**, *56*, 935−952.

(11) Hudson, B. S.; Kohler, B. E. A Low-Lying Weak Transition in the Polyene α,ω-Diphenyloctatetraene. *Chem. Phys. Lett.* **1972**, *14*, 299−304.

(12) Birge, R. R.; Schulten, K.; Karplus, M. Possible Influences of a Low-Lying "Covalent" Excited State on the Absorption Spectrum and Photoisomerization of 11-*cis* Retinal. *Chem. Phys. Lett.* **1975**, *31*, 451−454.

(13) Schulten, K.; Ohmine, J.; Karplus, M. Correlation Effects in the Spectra of Polyenes. *J. Chem. Phys.* **1976**, *64*, 4422−4441.

(14) Tavan, P.; Schulten, K. The Low-Lying Electronic Excitations in Long Polyenes: A PPP-MRD-CI Study. *J. Chem. Phys.* **1986**, *85*, 6602−6609.

(15) Tavan, P.; Schulten, K. Electronic Excitations in Finite and Infinite Polyenes. *Phys. Rev. B: Condens. Matter Mater. Phys.* **1987**, *36*, 4337−4358.

(16) Christensen, R. L.; Enriquez, M. M.; Wagner, N. L.; Peacock-Villada, A. Y.; Scriban, C.; Schrock, R. R.; Polívka, T.; Frank, H. A.; Birge, R. R. Energetics and Dynamics of the Low-Lying Electronic States of Constrained Polyenes: Implications for Infinite Polyenes. *J. Phys. Chem. A* **2013**, *117*, 1449−1465.

(17) Pendon, Z. D.; Sullivan, J. O.; van der Hoef, I.; Lugtenburg, J.; Cua, A.; Bocian, D. F.; Birge, R. R.; Frank, H. A. Stereoisomers of Carotenoids: Spectroscopic Properties of Locked and Unlocked *cis*-Isomers of Spheroidene. *Photosynth. Res.* **2005**, *86*, 5−24.

(18) Cerullo, G.; Polli, D.; Lanzani, G.; De Silvestri, S.; Hashimoto, H.; Cogdell, R. J. Photosynthetic Light Harvesting by Carotenoids: Detection of an Intermediate Excited State. *Science* **2002**, *298*, 2395−2398.

(19) Ostroumov, E. E.; Müller, M. G.; Marian, C. M.; Kleinschmidt, M.; Holzwarth, A. R. Electronic Coherence Provides a Direct Proof for Energy-Level Crossing in Photoexcited Lutein and β-Carotene. *Phys. Rev. Lett.* **2009**, *103*, 108302.

(20) Zhang, J.-P.; Inaba, Y.; Watanabe, Y.; Koyama, Y. Excited-State Dynamics Among the $1B_u^+$, $1B_u^-$ and $2A_g^-$ States of all-*trans*-Neurosporene as Revealed by Near-Infrared Time-Resolved Absorption Spectroscopy. *Chem. Phys. Lett.* **2000**, *332*, 351−358.

(21) Maiuri, M.; Polli, D.; Brida, D.; Lüer, L.; LaFountain, A. M.; Fuciman, M.; Cogdell, R. J.; Frank, H. A.; Cerullo, G. Solvent-Dependent Activation of Intermediate Excited States in the Energy Relaxation Pathways of Spheroidene. *Phys. Chem. Chem. Phys.* **2012**, *14*, 6312−6319.

(22) Koyama, Y.; Rondonuwu, F. S.; Fujii, R.; Watanabe, Y. Light-Harvesting Function of Carotenoids in Photo-Synthesis: The Roles of the Newly Found $1^1B_u^-$ State. *Biopolymers* **2004**, *74*, 2−18.

(23) Sashima, T.; Koyama, Y.; Yamada, T.; Hashimoto, H. The $1B_u^+$, $1B_u^-$, and $2A_g^-$ Energies of Crystalline Lycopene, β-Carotene, and Mini-9-β-Carotene as Determined by Resonance-Raman Excitation Profiles: Dependence of the $1B_u^-$ State Energy on the Conjugation Length. *J. Phys. Chem. B* **2000**, *104*, 5011−5019.

(24) Rondonuwu, F. S.; Watanabe, Y.; Zhang, J.-P.; Furuichi, K.; Koyama, Y. Internal-Conversion and Radiative-Transition Processes among the $1B_u^+$, $1B_u^-$ and $2A_g^-$ States of all-*trans*-Neurosporene as Revealed by Subpicosecond Time-Resolved Raman Spectroscopy. *Chem. Phys. Lett.* **2002**, *357*, 376−384.

(25) Rondonuwu, F. S.; Kakitani, Y.; Tamura, H.; Koyama, Y. Singlet Internal Conversion Processes in the Order of $1B_u^+ \rightarrow 3A_g^- \rightarrow 1B_u^- \rightarrow 2A_g^- \rightarrow 1A_g^-$ in all-*trans*-Spheroidene and Lycopene as Revealed by Subpicosecond Time-Resolved Raman Spectroscopy. *Chem. Phys. Lett.* **2006**, *429*, 234−238.

(26) Sashima, T.; Nagae, H.; Kuki, M.; Koyama, Y. A New Singlet-Excited State of all-*trans*-Spheroidene as Detected by Resonance-Raman Excitation Profiles. *Chem. Phys. Lett.* **1999**, *299*, 187−194.

(27) Shima, S.; Ilagan, R. P.; Gillespie, N.; Sommer, B. J.; Hiller, R. G.; Sharples, F. P.; Frank, H. A.; Birge, R. R. Two-Photon and Fluorescence Spectroscopy and the Effect of Environment on the Photochemical Properties of Peridinin in Solution and in the Peridinin-Chlorophyll-Protein from *Amphidinium carterae*. *J. Phys. Chem. A* **2003**, *107*, 8052−8066.

(28) Polívka, T.; Sundström, V. Dark Excited States of Carotenoids: Consensus and Controversy. *Chem. Phys. Lett.* **2009**, *477*, 1−11.

(29) Bautista, J. A.; Hiller, R. G.; Sharples, F. P.; Gosztola, D.; Wasielewski, M.; Frank, H. A. Singlet and Triplet Energy Transfer in the Peridinin-Chlorophyll *a*-Protein from *Amphidinium carterae*. *J. Phys. Chem. A* **1999**, *103*, 2267−2273.

(30) Zigmantas, D.; Hiller, R. G.; Sundström, V.; Polívka, T. Carotenoid to Chlorophyll Energy Transfer in the Peridinin−Chlorophyll-*a*−Protein Complex Involves an Intramolecular Charge Transfer State. *Proc. Natl. Acad. Sci. U. S. A.* **2002**, *99*, 16760−16765.

(31) Krueger, B. P.; Lampoura, S. S.; van Stokkum, I. H. M.; Papagiannakis, E.; Salverda, J. M.; Gradinaru, C. C.; Rutkauskas, D.; Hiller, R. G.; van Grondelle, R. Energy Transfer in the Peridinin Chlorophyll-*a* Protein of *Amphidinium carterae* Studied by Polarized Transient Absorption and Target Analysis. *Biophys. J.* **2001**, *80*, 2843−2855.

(32) Greco, J. A.; LaFountain, A. M.; Kinashi, N.; Shinada, T.; Sakaguchi, K.; Katsumura, S.; Magdaong, N. M.; Niedzwiedzki, D. M.; Birge, R. R.; Frank, H. A. Spectroscopic Investigation of the Carotenoid Deoxyperidinin: Direct Observation of the Forbidden $S_0 \rightarrow S_1$ Transition. *J. Phys. Chem. B* **2016**, *120*, 2731−2744.

(33) Englman, R.; Jortner, J. The Energy Gap Law for Radiationless Transitions in Large Molecules. *Mol. Phys.* **1970**, *18*, 145−164.

(34) Chynwat, V.; Frank, H. A. The Application of the Energy Gap Law to the S_1 Energies and Dynamics of Carotenoids. *Chem. Phys.* **1995**, *194*, 237−244.

(35) Frank, H. A.; Cua, A.; Chynwat, V.; Young, A.; Gosztola, D.; Wasielewski, M. R. The Lifetimes and Energies of the First Excited Singlet States of Diadinoxanthin and Diatoxanthin: The Role of These Molecules in Excess Energy Dissipatin in Algae. *Biochim. Biophys. Acta, Bioenerg.* **1996**, *1277*, 243−252.

(36) Frank, H. A.; Desamero, R. Z. B.; Chynwat, V.; Gebhard, R.; van der Hoef, I.; Jansen, F. J.; Lugtenburg, J.; Gosztola, D.; Wasielewski, M. R. Spectroscopic Properties of Spheroidene Analogs Having Different Extents of π-Electron Conjugatin. *J. Phys. Chem. A* **1997**, *101*, 149−157.

(37) Kosumi, D.; Yanagi, K.; Fujii, R.; Hashimoto, H.; Yoshizawa, M. Conjugation Length Dependence of Relaxation Kinetics in β-Carotene

DOI: 10.1021/acs.jpca.7b10001
J. Phys. Chem. A 2018, 122, 130−139

Homologs Probed by Femtosecond Kerr-Gate Fluorescence Spectroscopy. *Chem. Phys. Lett.* **2006**, *425*, 66−70.
(38) Krueger, B. P.; Scholes, G. D.; Fleming, G. R. Calculation of Couplings and Energy-Transfer Pathways between the Pigments of LH2 by the *ab Initio* Transition Density Cube Method. *J. Phys. Chem. B* **1998**, *102*, 5378−5386.
(39) Krueger, B. P.; Scholes, G. D.; Jimenez, R.; Fleming, G. R. Electronic Excitation Transfer from Carotenoid to Bacteriochloropyll in the Purple Bacterium *Rhodopseudomonas acidophila*. *J. Phys. Chem. B* **1998**, *102*, 2284−2292.
(40) Polívka, T.; Sundström, V. Ultrafast Dynamics of Carotenoid Excited States - From Solution to Natural and Artificial Systems. *Chem. Rev.* **2004**, *104*, 2021−2071.
(41) Polli, D.; Cerullo, G.; Lanzani, G.; De Silvestri, S.; Hashimoto, H.; Cogdell, R. J. Carotenoid-Bacteriochlorophyll Energy Transfer in LH2 Complexes Studied with 10-fs Time Resolution. *Biophys. J.* **2006**, *90*, 2486−2497.
(42) Cong, H.; Niedzwiedzki, D. M.; Gibson, G. N.; LaFountain, A. M.; Kelsh, R. M.; Gardiner, A. T.; Cogdell, R. J.; Frank, H. A. Ultrafast Time-Resolved Carotenoid to-Bacteriochlorophyll Energy Transfer in LH2 Complexes from Photsynthetic Bacteria. *J. Phys. Chem. B* **2008**, *112*, 10689−10703.
(43) Wohlleben, W.; Buckup, T.; Herek, J. L.; Cogdell, R. J.; Motzkus, M. Multichannel Carotenoid Deactivation in Photosynthetic Light Harvesting as Identified by an Evolutionary Target Analysis. *Biophys. J.* **2003**, *85*, 442−450.
(44) Kleinschmidt, M.; Marian, C. M.; Waletzke, M.; Grimme, S. Parallel Multireference Configuration Interaction Calculations on Mini-β-Carotenes and β-Carotene. *J. Chem. Phys.* **2009**, *130*, 044708−1−044798−11.
(45) Starcke, J. H.; Wormit, M.; Schirmer, J.; Dreuw, A. How Much Double Excitation Character Do the Lowest Excited States of Linear Polyenes Have? *Chem. Phys.* **2006**, *329*, 39−49.
(46) Dreuw, A.; Head-Gordon, M. Single-Reference *ab Initio* Methods for the Calculation of Excited States of Large Molecules. *Chem. Rev.* **2005**, *105*, 4009−4037.
(47) Ghosh, D.; Hachmann, J.; Yanai, T.; Chan, G. K.-L. Orbital Optimization in the Density Matrix Renormalization Group, with Applications to Polyenes and β-Carotene. *J. Chem. Phys.* **2008**, *128*, 144117−1−144117−14.
(48) Marian, C. M.; Gilka, N. Performance of the Density Functional Theory/Multireference Configuration Interaction Method on Electronic Excitation of Extended π-Systems. *J. Chem. Theory Comput.* **2008**, *4*, 1501−1515.
(49) Schmidt, M.; Tavan, P. Electronic Excitations in Long Polyenes Revisted. *J. Chem. Phys.* **2012**, *136*, 124309−1−124309−13.
(50) Koyama, Y.; Kakitani, Y.; Miki, T.; Christiana, R.; Nagae, H. Excited-State Dynamics of Overlapped Optically-Allowed $1B_u^+$ and Optically Forbidden $1B_u^-$ or $3A_g^-$ Vibronic Levels of Carotenoids: Possible Roles in the Light-Harvesting Function. *Int. J. Mol. Sci.* **2010**, *11*, 1888−1929.
(51) Fujii, R.; Inaba, Y.; Watanabe, Y.; Koyama, K.; Zhang, J.-P. Two Different Pathways of Internal Conversion in Carotenoids Depending on the Length of the Conjugated Chain. *Chem. Phys. Lett.* **2003**, *369*, 165−172.
(52) Fujii, R.; Fujino, T.; Inaba, Y.; Nagae, H.; Koyama, Y. Internal Conversion of $1B_u^+ \rightarrow 1B_u^- \rightarrow 2A_g^-$ and Fluorescence from the $1B_u^-$ State in all-*trans*-Neurosporene as Probed by Up-Conversion Spectroscopy. *Chem. Phys. Lett.* **2004**, *384*, 9−15.
(53) Polli, D.; Cerullo, G.; Lanzani, G.; De Silvestri, S.; Yanagi, K.; Hashimoto, H.; Cogdell, R. J. Conjugation Length Dependence of Internal Conversion in Carotenoids: Role of the Intermediate State. *Phys. Rev. Lett.* **2004**, *93*, 163002.
(54) Rondonuwu, F. S.; Watanabe, Y.; Fujii, R.; Koyama, Y. A First Detection of Singlet to Triplet Conversion from the $1^1B_u^-$ to the 1^3A_g State and Triplet Internal Conversion from the 1^3A_g to the 1^3B_u State in Carotenoids: Dependence on the Conjugation Length. *Chem. Phys. Lett.* **2003**, *376*, 292−301.
(55) Kobayashi, T.; Nishimura, K.; Rondonuwu, F. S.; Koyama, Y. Excited-State Dynamics of the $1B_u^+$, $3A_g^-$, and $1B_u^-$ States in a Carotenoid Molecule by 5-fs Absorption Spectroscopy. *J. Lumin.* **2005**, *112*, 391−394.
(56) Sutresno, A.; Kakitani, Y.; Zuo, P.; Li, C.; Koyama, Y.; Nagae, H. Presence and Absence of Electronic Mixing in Shorter-Chain and Longer-Chain Carotenoids: Assignment of the Symmetries of $1B_u^-$ and $3A_g^-$ States Located Just Below the $1B_u^+$ State. *Chem. Phys. Lett.* **2007**, *447*, 127−133.
(57) Ostroumov, E. E.; Mulvaney, R. M.; Cogdell, R. J.; Scholes, G. D. Broadband 2D Electronic Spectroscopy Reveals a Carotenoid Dark State in Purple Bacteria. *Science* **2013**, *340*, 52−56.
(58) Herzberg, G.; Teller, E. Vibrational Structure of Electronic Transitions in Polyatomic Molecules. *Z. Phys. Chem., Abt. B* **1933**, *21*, 410−446.
(59) Geldof, P. A.; Rettschnick, R. P. H.; Hoytink, G. J. Vibronic Coupling and Radiative Transitions. *Chem. Phys. Lett.* **1971**, *10*, 549−558.
(60) McClure, D. S. Excited States of the Naphthalene Molecule. I. Symmetry Properties of the First Two Excited Singlet States. *J. Chem. Phys.* **1954**, *22*, 1668−1675.
(61) Yoshizawa, M.; Kosumi, D.; Komukai, M.; Hashimoto, H. Ultrafast Optical Responses of Three-Level Systems in β-Carotene: Resonance to a High-Lying $n^1A_g^-$ Excited State. *Laser Phys.* **2006**, *16*, 325−330.
(62) Yoshizawa, M.; Aoki, K.; Hashimoto, H. Vibrational Relaxation of the $2A_g^-$ Excited State in all-*trans*-β-Carotene Obtained by Femtosecond Time-Resolved Raman Spectroscopy. *Phys. Rev. B: Condens. Matter Mater. Phys.* **2001**, *63*, 180301.
(63) McCamant, D. W.; Kukura, P.; Mathies, R. A. Femtosecond Time-Resolved Stimulated Raman Spectroscopy: Application to the Ultrafast Internal Conversion of β-Carotene. *J. Phys. Chem. A* **2003**, *107*, 8208−8214.
(64) McCamant, D. W.; Kim, J. E.; Mathies, R. A. Vibrational Relaxation in B-Carotene Probed by Picosecond Stokes and Anti-Stokes Resonance Raman Spectroscopy. *J. Phys. Chem. A* **2002**, *106*, 6030−6038.
(65) Shim, S.; Mathies, R. A. Development of a Tunable Femtosecond Stimulated Raman Apparatus and Its Application to β-Carotene. *J. Phys. Chem. B* **2008**, *112*, 4826−4832.
(66) Buckup, T.; Hauer, J.; Möhring, J.; Motzkus, M. Multidimensional Spectroscopy of β-Carotene: Vibrational Cooling in the Excited State. *Arch. Biochem. Biophys.* **2009**, *483*, 219−223.
(67) Wohlleben, W.; Buckup, T.; Hashimoto, H.; Cogdell, R. J.; Herek, J. L.; Motzkus, M. Pump-Deplete-Probe Spectroscopy and the Puzzle of Carotenoid Dark States. *J. Phys. Chem. B* **2004**, *108*, 3320−3325.
(68) Ghosh, S.; Bishop, M. M.; Roscioli, J. D.; Mueller, J. J.; Shepherd, N. C.; LaFountain, A. M.; Frank, H. A.; Beck, W. F. Femtosecond Heterodyne Transient-Grating Studies of Nonradiative Decay of the $S_2(1^1B_u^+)$ State of β-Carotene: Contributions from Dark Intermediates and Double-Quanum Coherences. *J. Phys. Chem. B* **2015**, *119*, 14905−14924.
(69) Ghosh, S.; Roscioli, J. D.; Bishop, M. M.; Gurchiek, J. K.; LaFountain, A. M.; Frank, H. A.; Beck, W. F. Torsional Dynamics and Intramolecular Charge Transfer in the $S_2(1^1B_u^+)$ Excited State of Peridinin: A Mechanism for Enhanced Mid-Visible Light Harvesting. *J. Phys. Chem. Lett.* **2016**, *7*, 3621−3626.
(70) Beck, W. F.; Bishop, M. M.; Roscioli, J. D.; Ghosh, S.; Frank, H. A. Excited State Conformational Dynamics in Carotenoids: Dark Intermediates and Excitation Energy Transfer. *Arch. Biochem. Biophys.* **2015**, *572*, 175−183.
(71) Hauer, J.; Buckup, T.; Motzkus, M. Pump-Degenerate Four Wave Mixing as a Technique for Analyzing Structural and Electronic Evolution: Multidimensional Time-Resolved Dynamics near a Conical Intersection. *J. Phys. Chem. A* **2007**, *111*, 10517−10529.
(72) Hauer, J.; Buckup, T.; Motzkus, M. Quantum Control Spectroscopy of Vibrational Modes: Comparison of Control Scenarios

DOI: 10.1021/acs.jpca.7b10001
J. Phys. Chem. A 2018, 122, 130−139

for Ground and Excited States in β-Carotene. *Chem. Phys.* **2008**, *350*, 220−229.
(73) Sugisaki, M.; Yanagi, K.; Cogdell, R. J.; Hashimoto, H. Unified Explanation for Linear and Nonlinear Optical Responses in β-Carotene: A Sub-20-fs Degenerate Four-Wave Mixing Spectroscopic Study. *Phys. Rev. B: Condens. Matter Mater. Phys.* **2007**, *75*, 15510.
(74) Sugisaki, M.; Fujiwara, M.; Yanagi, K.; Cogdell, R. J.; Hashimoto, H. Four-Wave Mixing Signals from β-Carotene and Its n = 15 Homologue. *Photosynth. Res.* **2008**, *95*, 299−308.
(75) Fujiwara, M.; Yamauchi, K.; Sugisaki, M.; Gall, A.; Robert, B.; Cogdell, R. J.; Hashimoto, H. Energy Dissipation in the Ground-State Vibrational Manifolds of β-Carotene Homologues: A Sub-20-fs Time-Resolved Transient Grating Spectroscopic Study. *Phys. Rev. B: Condens. Matter Mater. Phys.* **2008**, *77*, 205118.
(76) Christensson, N.; Polívka, T.; Yartsev, A.; Pullerits, T. Photon Echo Spectroscopy Reveals Structure-Dynamics Relationships in Carotenoids. *Phys. Rev. B: Condens. Matter Mater. Phys.* **2009**, *79*, 245118.
(77) Oliver, T. A. A.; Fleming, G. R. Following Coupled Electronic-Nuclear Motion through Conical Intersections in the Ultrafast Relaxation of β-Apo-8′-Carotenal. *J. Phys. Chem. B* **2015**, *119*, 11428−11441.
(78) Enriquez, M. M.; Hananoki, S.; Hasegawa, S.; Kajikawa, T.; Katsumura, S.; Wagner, N. L.; Birge, R. R.; Frank, H. A. Effect of Molecular Symmetry on the Spectra and Dynamics of the Intramolecular Charge Transfer (ICT) State of Peridinin. *J. Phys. Chem. B* **2012**, *116*, 10748−10756.
(79) Martinson, T. A.; Plumley, F. G. One-Step Extraction and Concentration of Pigments and Acyl Lipids by Sec-Butanol from *in Vitro* and *in Vivo* Samples. *Anal. Biochem.* **1995**, *228*, 123−130.
(80) Hananoki, S. Synthesis of Ylidenebutenolide-Shift Compounds of Peridinin, Carotenoid, Directing Toward Elucidating the Super-Efficient Energy Transfer Mechanism of Peridinin. M.S., Kwansei Gakuin University, Hyogo, Japan, 2012.
(81) Frisch, M. J.; Trucks, G. W.; Schlegel, H. B.; Scuseria, G. E.; Robb, M. A.; Cheeseman, J. R.; Scalmani, G.; Barone, V.; Mennucci, B.; Petersson, G. A. et al. *Gaussian 09*, revision C.01; Gaussian, Inc.: Wallingford, CT, 2009.
(82) Stanton, J. F.; Bartlett, R. J. Equation of Motion Coupled-Cluster Method: A Systematic Biorthogonal Approach to Molecular Excitation Energies, Transition Probabilities, and Excited State Properties. *J. Chem. Phys.* **1993**, *98*, 7029−7039.
(83) Koch, H.; Kobayashi, R.; Sánchez de Merás, A.; Jørgensen, P. Calculation of Size-Intensive Transition Moments from the Coupled Cluster Singles and Doubles Linear Response Function. *J. Chem. Phys.* **1994**, *100*, 4393−4400.
(84) Kállay, M.; Gauss, J. Calculation of Excited-State Properties Using General Coupled-Cluster and Configuration-Interaction Models. *J. Chem. Phys.* **2004**, *121*, 9257−9269.
(85) Wagner, N. L.; Greco, J. A.; Enriquez, M. M.; Frank, H. A.; Birge, R. R. The Nature of the Intramolecular Charge Transfer State in Peridinin. *Biophys. J.* **2013**, *104*, 1314−1325.
(86) Bovi, D.; Mezzetti, A.; Vuilleumier, R.; Gaigeot, M.-P.; Chazallon, B.; Spezia, R.; Guidoni, L. Environmental Effects on Vibrational Properties of Carotenoids: Experiments and Calculations on Peridinin. *Phys. Chem. Chem. Phys.* **2011**, *13*, 20954−20964.
(87) Martin, C. H.; Birge, R. R. Reparameterizing MNDO for Excited State Calculations Using *ab Initio* Effective Hamiltonian Theory: Application to the 2,4-Pentadien-1-iminium Cation. *J. Phys. Chem. A* **1998**, *102*, 852−860.
(88) Niedzwiedzki, D. M.; Chatterjee, N.; Enriquez, M. M.; Kajikawa, T.; Hasegawa, S.; Katsumura, S.; Frank, H. A. Spectroscopic Investigation of Peridinin Analogues Having Different π-Electron Conjugated Chain Lengths: Exploring the Nature of the Intramolecular Charge Transfer State. *J. Phys. Chem. B* **2009**, *113*, 13604−13612.
(89) Krylov, A. I. Equation-of-Motion Coupled-Cluster Methods for Open-Shell and Electronically Excited Species: The Hitchhiker's Guide to Fock Space. *Annu. Rev. Phys. Chem.* **2008**, *59*, 433−462.
(90) Head-Gordon, M.; Pople, J. A.; Frisch, M. J. MP2 Energy Evaluation by Direct Methods. *Chem. Phys. Lett.* **1988**, *153*, 503−506.
(91) Dunning, T. H.; Hay, P. J. Modern Theoretical Chemistry. In *Modern Theoretical Chemistry*; Schaefer, H. F., Ed.; Plenum: New York, 1976; Vol. 3, pp 1−28.

DOI: 10.1021/acs.jpca.7b10001
J. Phys. Chem. A 2018, 122, 130−139